Sustainable Food Proteins

WILEY

AOCS Your Global Fats and Oils Connection

ORIGINAL ARTICLE OPEN ACCESS

Pea Flours Display Wide-Ranging Intrinsic Physicochemical and Functional Traits Affecting Their Role as Food Ingredients

Emma D. Matzen[1,2] | Mette S. Mikkelsen[2] | Julian D. McClements[3] | Lutz Grossmann[3]

[1]Department of Food Science, University of Copenhagen, Frederiksberg, Denmark | [2]FOSS, Hilleroed, Denmark | [3]Department of Food Science, University of Massachusetts Amherst, Amherst, Massachusetts, USA

Correspondence: Lutz Grossmann (lkgrossmann@umass.edu)

Received: 30 July 2025 | **Revised:** 8 January 2026 | **Accepted:** 8 January 2026

Keywords: functional proteins | legume protein | NIR | pea protein | pea starch | *Pisum* | plant-based | plant protein | pulse protein | sustainable foods

ABSTRACT

Unrefined pea (*Pisum sativum*) flour is a promising food material that can either serve as a functional standalone ingredient or as the starting material to extract functional proteins and starches. This observational study used rapid screening of 650 pea accessions, which span a domestication range from wild species to modern cultivars, to select 20 representative samples based on near-infrared spectral differences, capturing broad compositional diversity and illustrating how intrinsic physicochemical and protein functional traits influence their suitability in foods. To investigate the intrinsic variability, the physicochemical properties (surface charge, thermal properties, particle size), functional characteristics (solubility, interfacial tension), and visual characteristics were analyzed. Small variations in surface charge conditions were found at pH 5 and 7, whereas the charge varied from 2.7 ± 1.4 to 11.5 ± 1.4 mV at pH 3. However, high variations were found in protein solubility that ranged from 28.4% ± 5.1% to 92.2% ± 1.5% at pH 7, and differences in protein characteristics were also identified in thermal denaturation temperatures that ranged from 85.2°C ± 0.2°C to 99.6°C ± 0.8°C. These observations were confirmed through microstructural characterizations that also showcased the intrinsic color and size differences of the main constituents (starch granules and protein bodies). The findings of this study indicate that there are significant variations in the physicochemical and functional properties of different pea flours, which have considerable potential for the food industry. This highlights the importance of selecting the appropriate pea raw materials for optimal results in various food applications.

1 | Introduction

Plant proteins are sustainable food ingredients (Grossmann 2023; Zhao et al. 2020). Especially the field pea '*Pisum sativum*' has attracted much attention over the last decade, and pea protein ingredients (flours, concentrates, and isolates) are frequently used to formulate foods such as plant-based meats or dairy alternatives (Ding Tao et al. 2023; Santos et al. 2019). The reason is that peas are known for their minimal allergenicity and their relatively high protein quality with a digestible indispensable amino acid score (DIAAS) of up to 1.0 (Guillin et al. 2022).

Production of quality foods with high consumer acceptance requires a consistent composition and quality of the raw materials (Liu et al. 2023). Several studies indicated that there are substantial fluctuations in the quality parameters of pea protein ingredients depending on their extraction procedure, resulting in changes in their functional attributes (Hansen et al. 2022). For example, Tanger et al. (2020) reported different solubility profiles when pea proteins were extracted using salt, micellar (i.e., formation of insoluble pellets), and alkali-isoelectric point precipitation. Moreover, the solubility profiles obtained through these different lab-scale extraction methods were very different

This is an open access article under the terms of the Creative Commons Attribution License, which permits use, distribution and reproduction in any medium, provided the original work is properly cited.

© 2026 The Author(s). *Sustainable Food Proteins* published by American Oil Chemists' Society and Wiley Periodicals LLC.

compared to a commercial sample. The commercial sample exhibited very low solubility (< 10% over the pH range 3 to 8). In contrast, the samples prepared by the authors showed high solubility in the acidic as well as neutral to alkaline pH range, which was also observed by Hansen et al. (2022). Differences like these may stem from unfavorable processing conditions such as pH and temperature, leading to protein denaturation and aggregation, ultimately altering protein functionality such as emulsification, foaming, gelation, and digestibility (Chao and Aluko 2018; Shand et al. 2007).

The studies mentioned above mainly focused on how different extraction procedures and conditions affect the molecular, physicochemical, and functional properties of pea ingredients. The studies are typically based on randomly selected pea seeds or pea flours, and the natural variability of different pea accessions is typically not considered. Accessions are defined as "[...] uniquely identifiable sample of seeds representing a cultivar, breeding line or a population [...]" (FAO 2018). However, it is well known that the composition of plant seeds is affected by internal (i.e., genetic makeup) and external (i.e., cultivation conditions) parameters (Chen et al. 2023; Mertens et al. 2012). Especially, the differences in functional and physicochemical properties between different pea accessions have not been well studied yet. Previous studies mainly looked into the proximate composition of different pea accessions and revealed considerable differences between the individual seeds (Choi et al. 2022; Kotlarz et al. 2011; Taghvaei et al. 2022; Vidal-Valverde et al. 2003). For example, Choi et al. (2022) revealed that the protein content of 62 pea accessions ranges from 169.0 to 230.3 $g\,kg^{-1}$. Moreover, other studies focused on investigating the physicochemical and functional properties (e.g., solubility, foaming, emulsification) of pea proteins isolated from different pea accessions and generally showed that these properties vary between pea samples (Garcia Arteaga et al. 2021; Lam et al. 2016). This highlights the need for selecting the right pea raw materials when it comes to tailoring ingredients toward specific applications.

However, these studies examined the variance in protein properties arising from isolated compounds, leaving a gap in comprehensive research on the functional attributes of unrefined pea flours. This is despite recent research indicating that pea flour might exhibit comparable functional properties to isolated compounds, offering potential benefits for incorporating minimally processed pea flour as a functional ingredient into foods (Hall and Moraru 2021). Moreover, less-refined ingredients are generally associated with a lower environmental footprint. Studies on yellow peas show that aqueous fractionation reduces all environmental impact indicators by approximately 30%–40% compared to state-of-the-art fractionation methods, with reduced impacts also evident when expressed on a protein basis (Lie-Piang et al. 2021). However, flours may exhibit even lower environmental impacts, as no fractionation is required, thereby minimizing energy inputs and avoiding material losses. Beyond serving as a standalone food ingredient for specific applications, pea flour is the starting material to extract functional proteins, and therefore selecting the right flour is crucial to obtain an ingredient with the desired properties. With the increase in pea protein consumption, there is an opportunity to further investigate the physicochemical or functional properties of pea flours and find novel pea accessions that might have unique physicochemical or functional properties that can then be cultivated on a larger scale in the future. This could enable the discovery of flours with high functionality, eliminating the need for extensive downstream processing to isolate specific compounds from the seed, thus offering potential benefits in terms of water and energy conservation (Lie-Piang et al. 2021).

The goal of this observational study was to show how rapid screening can uncover compositional differences among pea accessions. Out of 650 accessions, 20 representative flour samples were selected to reflect the wide range in composition and to highlight differences in physicochemical and protein functional properties, demonstrating how intrinsic traits shape their suitability for use in foods.

2 | Materials and Methods

2.1 | Materials

The pea seeds used in this study were supplied by The Nordic Genetic Resource Center (NordGen, Alnarp, Sweden). NordGen possesses a diverse collection of seeds originating from the Nordic countries. The collection spans a wide range of pea varieties and domestication levels. All accessions used in this study can be ordered from NordGen (https://www.nordgen.org).

The pea seeds underwent drying post-harvest at a relative humidity of 150 $g\,kg^{-1}$ until they attained a moisture content of a maximum of 80 $g\,kg^{-1}$. They were subsequently stored at −18°C in three-layered aluminum bags to minimize moisture exchange. Thawing was carried out at ambient temperature. All other chemicals used in this study were of analytical grade and obtained through VWR (Radnor, PA, USA).

2.2 | Methods

2.2.1 | Selection of Pea Accessions

Six hundred fifty pea accessions were screened in reflectance mode using a FOSS NIRS DS3 (FOSS Analytical, Hilleroed, Denmark). In the instrument, a light bulb emits light at wavelengths ranging from 400 to 2500 nm into the sample. The light reflects from the sample toward a detector. The detector registers the intensity of the light at different wavelengths reflected from the sample, creating an absorbance spectrum representing the chemical fingerprint of the sample (Osborne et al. 1993). For the measurements, the pea seeds were placed in a measuring cup at ambient temperature. Each spectrum obtained was created from an average of seven sub-scans. To ensure representative measurements, the pea seeds were mixed in the vessel between each of the three replicate scans. The spectra were analyzed using MATLAB (R2022b, MathWorks, Natick, USA) and PLS_Toolbox (version 9.2 (2024), Eigenvector Research, Manson, USA). Two pre-processing methods were applied to the spectral data: Standard normal variate and mean centering to reduce the noise and the baseline effect in the spectra (Tomasi et al. 2004).

Principal component analysis (PCA) was performed to visualize differences in the spectral profiles of the pea seeds. Based on the PCA, 20 pea accessions representative of the spectral variation of the pea seed collection were selected for the present study (see section 3.1), which also had different geographical origins (Table S1). This selection was performed based on the placement of a score in the score plot since grouped scores share a common feature with the principal component, while scores opposite in the score plot are negatively correlated (Bro and Smilde 2014). The 20 selected pea accessions were therefore chosen to cover all underlying relations referring to their spectral and compositional differences. The overall approach is shown in Figure 1.

2.2.1.1 | Compositional Analysis of Whole Peas

2.2.1.1.1 | Protein. The protein content was determined with the Dumas method (Dumatec 8000, FOSS Analytical, Hilleroed, Denmark) according to the official reference method ISO 16634 (FOSS Analytical 2019). The nitrogen content was multiplied by a protein factor of 5.36 (François Mariotti and Mirand 2008).

2.2.1.1.2 | Total Lipids. The lipid content was determined according to ISO 11085 by initially hydrolyzing (Hydrotec 8000, FOSS Analytical, Hilleroed, Denmark) the pea flour with hydrochloric acid for 2 h (FOSS Analytical 2018a). The lipid extraction (Soxtec 8000, FOSS Analytical, Hilleroed, Denmark) was performed using petroleum ether for 1 h (FOSS Analytical 2018b).

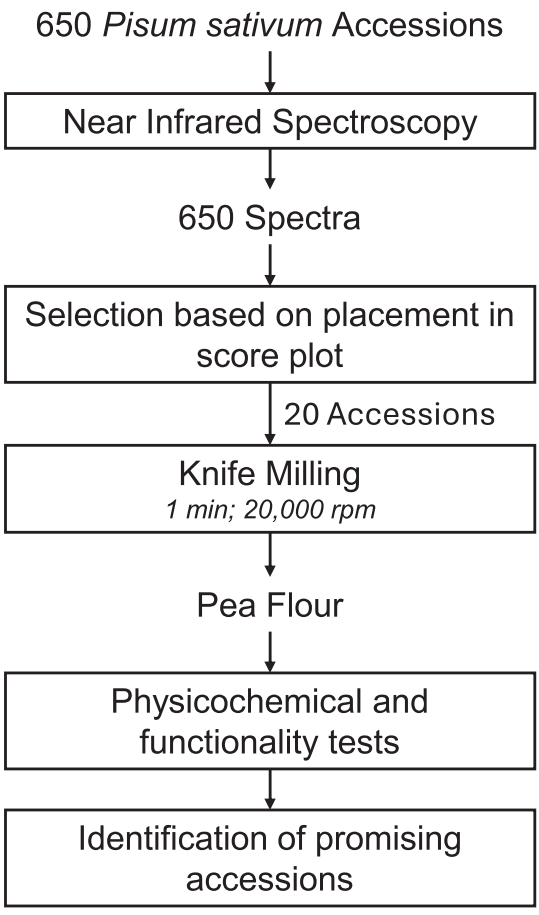


FIGURE 1 | Experimental flowchart that displays how the pea flours were analyzed.

2.2.1.1.3 | Starch. The AOAC Method 996.11—specifically K-TSTA-100A was used to determine the total starch (α-amylase/amyloglucosidase) (Megazyme 2024).

2.2.1.1.4 | Ash. The ash content was determined by the ICC Standard No. 104/1. A Muffle furnace (Nabertherm GmbH, Lilienthal, Germany) was used for the heat treatment, and a desiccator containing silica gel for the cooling (ICC 1990).

2.2.2 | Physicochemical and Functional Properties

2.2.2.1 | Flour Preparation. Thirty grams of each pea accession was milled using a knife mill (IKA MultiDrive control, IKA-Werke GmbH & Co. KG, Staufen, Germany) for 1 min at 20,000 rpm. The vessel was cooled during the process, which ensured product temperatures < 30°C. The resulting flours were transferred into moisture-sealed containers and stored at 4°C until further use.

2.2.2.2 | Solution Preparation. Pea flour and deionized water dispersions were prepared at the required concentration and stirred for 30 min until the flour was completely dispersed. In case further homogenization was needed, the solutions were homogenized (Ultra Turrax, IKA-Werke GmbH & Co. KG, Staufen, Germany) at 15,000 rpm for 2 min. Flour solutions were adjusted to the required pH (3, 5, or 7, depending on the method) with HCL and NaOH (0.1–1 M and 0.05–0.5 M) using a calibrated pH meter (pHenomenal pH 1100 L, VWR International, Pennsylvania, USA). The pH was monitored for 30 min before the samples were transferred for overnight storage at 4°C and readjusted with an accuracy of ±0.1 the next day at room temperature if necessary.

2.2.2.3 | Zeta Potential. To reveal the difference in surface charge at different pH values, the zeta potential (Zetasizer Nano Z2, Malvern Instruments Ltd., Malvern, Worcestershire, UK) was measured. Homogenized solutions with a concentration of 10 g kg^{-1} were used to achieve an optimum signal. If needed, the solutions were diluted with a phosphate–citrate buffer at the respective pH values (Rex et al. 1989). The folded capillary cells (Malvern Instruments Ltd., Malvern, Worcestershire, UK) were rinsed first with the buffer at the target pH and then with the solution before being refilled with the sample solution. The ζ-potential was determined by measuring the direction and velocity that the droplets moved in the electric field applied, and the Smoluchowski equation was utilized to calculate the ζ-potential.

2.2.2.4 | Thermal Properties. Differential scanning calorimetry (DSC) was used to identify the starch gelation and protein denaturation temperatures. For this, solutions containing 350 g kg^{-1} pea flour were prepared without homogenizing. In addition, to distinguish between the protein and starch peaks, the protein was isolated from the flour. Three accessions were selected based on the differences in placement and magnitude of the enthalpy peaks. For this, 100 g kg^{-1} pea flour solutions were stirred with a magnetic stirrer for 2 h with pH adjustments to pH 8 using 1 M NaOH every 30 min. The solutions were centrifuged for 20 min at 4500 × *g* to separate the starch-rich fraction (pellet) from the protein-rich fraction (supernatant). The protein in the supernatant was subsequently precipitated at pH 4.5 and separated by centrifugation

for 20 min at 4500 × *g*. All samples were subsequently adjusted to pH 7 before DSC analysis.

All samples were measured in 100 μL aluminum pans that were hermetically sealed before analysis (TA DSC25, TA Instruments, New Castle, USA). Each sample was heated from 25°C to 105°C at a heating rate of 3°C/min. All samples were measured twice, and the results were analyzed with the TRIOS software (TA Instruments, New Castle, USA).

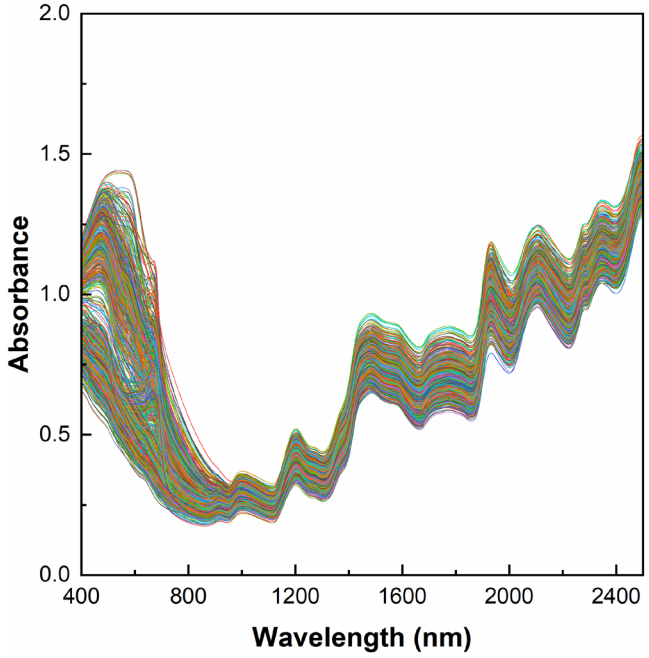


FIGURE 2 | Raw spectral data derived from NIR spectra of the 650 pea accessions. Nanometer (nm) is represented on the *x*-axis, and absorption intensity is represented on the *y*-axis. Different colors represent different samples.

2.2.2.5 | **Static Light Scattering.** To measure the particle size distribution, 10 g kg^{-1} pea flour solutions were prepared without homogenizing and measured using a Mastersizer 3000 (Malvern Instruments Ltd., Westborough, USA). A refractive index of 1.45 was chosen, and laser obscuration was around 6. The results are reported as weighted mean value by diameter ($D_{3,2}$) and weighted mean value by volume ($D_{4,3}$).

2.2.2.6 | **Protein Solubility.** The solutions analyzed consisted of 10 g kg^{-1} pea flour. To obtain a supernatant for all solutions, 1.5 mL was centrifuged (Multifuge X4, Thermo Fisher Scientific, Massachusetts, USA) for 15 min at 20,000 × *g*. The protein content of both the supernatant and the solutions before centrifugation was analyzed with the Dumas combustion method (Rapid MAX N, Elementar Analysensysteme GmbH, Langenselbold, Germany). The protein factor used for converting the nitrogen content was 5.36 (François Mariotti and Mirand 2008). The protein solubility was then calculated using Equation (1):

$$\text{Protein solubility} = c_{\text{protein,supernatant}} / c_{\text{protein,solution}} \quad (\%) \tag{1}$$

2.2.2.7 | **Surface Tension.** The dynamic surface tension of a 10 g kg^{-1} pea flour solution was measured in a bubble pressure tensiometer (BPT Mobile, Krüss, Hamburg, Germany), which assesses the highest internal pressure of a gas bubble generated in a liquid via capillary force at a constant bubble formation rate. The surface tension can then be calculated using the Young–Laplace equation. The number of steps was

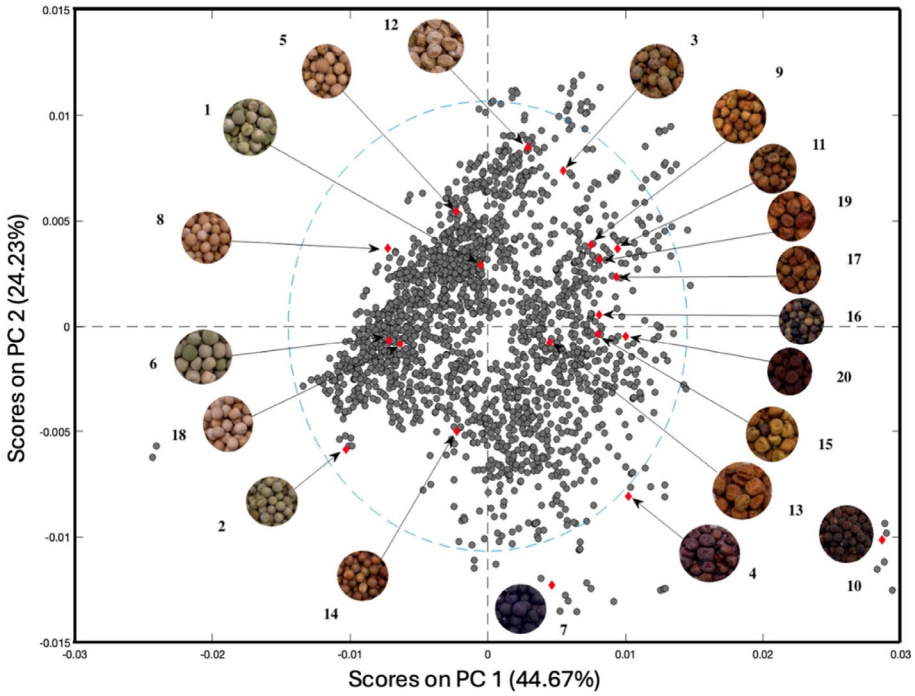


FIGURE 3 | Score plot derived from NIR spectra of the 650 pea accessions. PC1 is represented on the *x*-axis with an explained variance of 44.67% and PC2 is represented on the *y*-axis with an explained variance of 24.23%. The 20 selected pea accessions are represented with pea sample numbers and photos.

TABLE 1 | Chemical composition of 20 pea accessions with pictures of the pea seeds. Pea accession number provided according to Nordic Baltic Genebanks Information System (GeNBIS).

Pea sample		Pea accession	Protein (g kg^{-1} DM)	Fat (g kg^{-1} DM)	Starch (g kg^{-1} DM)	Ash (g kg^{-1} DM)
	1	NGB102401	172.9^{i} ± 0.4	18.4^{cd} ± 0.5	476.0^{ab} ± 4.0	25.9^{g} ± 0.1
	2	NGB11935	180.7^{hi} ± 1.9	23.2^{b} ± 0.1	439.7^{bcde} ± 3.7	32.5^{c} ± 0.4
	3	NGB20013	206.6^{defgh} ± 18.1	16.6^{cde} ± 0.1	444.7^{bcde} ± 12.5	24.3^{hi} ± 0.1
	4	NGB103830	201.3^{fghi} ± 0.6	17.1^{cde} ± 1.6	414.5^{ef} ± 8.7	28.5^{ef} ± 0.2
	5	NGB17833	178.3^{hi} ± 1.4	18.1^{cd} ± 0.1	501.2^{a} ± 10.3	22.9^{i} ± 0.6
	6	NGB8646	202.6^{efghi} ± 0.0	17.2^{cde} ± 0.3	471.2^{abc} ± 21.3	28.2^{ef} ± 0.0
	7	NGB106016	211.5^{defg} ± 1.6	17.8^{cd} ± 0.5	448.8^{bcde} ± 1.3	27.3^{f} ± 0.5
	8	NGB105418	218.1^{cdefg} ± 1.0	17.0^{cde} ± 0.2	458.5^{abcde} ± 17.5	34.5^{b} ± 0.1
	9	NGB103523	195.3^{ghi} ± 2.5	19.2^{c} ± 0.4	442.2^{bcde} ± 12.1	25.6^{gh} ± 0.0
	10	NGB101787	219.2^{cdefg} ± 1.2	12.7^{fgh} ± 0.9	375.6^{fg} ± 6.5	36.5^{a} ± 0.3
	11	NGB102149	230.9^{abcdef} ± 0.8	17.6^{cde} ± 0.2	427.1^{cde} ± 4.3	24.7^{gh} ± 0.8
	12	NGB20205	232.9^{abcde} ± 0.2	30.2^{a} ± 0.7	337.7^{g} ± 1.1	29.1^{de} ± 0.1

(Continues)

TABLE 1 | (Continued)

Pea sample		Pea accession	Protein (g kg^{-1} DM)	Fat (g kg^{-1} DM)	Starch (g kg^{-1} DM)	Ash (g kg^{-1} DM)
	13	NGB17869	236.9^{abcd} ± 3.7	18.1^{cd} ± 0.4	469.9^{abc} ± 11.9	30.3^{d} ± 0.5
	14	NGB102153	230.3^{abcdef} ± 1.6	14.4^{efg} ± 1.4	442.2^{bcde} ± 19.2	29.1^{de} ± 0.3
	15	NGB102222	242.6^{abc} ± 27.7	12.2^{h} ± 0.3	437.4^{bcde} ± 16.5	25.3^{gh} ± 0.2
	16	NGB24334	256.3^{a} ± 0.7	17.4^{cde} ± 0.1	416.5^{ef} ± 6.9	27.7^{f} ± 0.2
	17	NGB13784	222.8^{bcdef} ± 1.8	17.3^{cde} ± 0.6	448.2^{bcde} ± 3.7	25.7^{g} ± 0.5
	18	NGB102680	230.9^{abcedf} ± 3.5	15.8^{def} ± 0.3	464.0^{abcd} ± 0.2	27.9^{ef} ± 0.1
	19	NGB103050	250.9^{ab} ± 1.3	13.1^{gh} ± 0.4	448.8^{bcde} ± 5.1	25.7^{g} ± 0.2
	20	NGB100005	253.7^{a} ± 1.6	12.2^{h} ± 0.3	423.4^{de} ± 13.8	25.8^{g} ± 0.0

Note: Different lower-case superscripts indicate statistically significant differences in the same column ($p < 0.05$). The country of origin of the accessions can be found in Table S1.

set to $n = 30$ with a start surface age of 10 ms and a stop surface age of 30,000 ms. The measuring chamber was cleaned with ethanol before filling with the solution. The surface tension obtained from the pea flour solutions was compared at step number 30.

2.2.2.8 | Microstructure

2.2.2.8.1 | Light Microscopy. To visualize the microstructure of the pea flour solutions, light microscopy images were taken. About 10 g kg^{-1} pea flour solutions were visualized (BTW1-213, National Optical & Scientific Instruments, Texas, USA) with a 40× optic lens and photographed (Motic camera BTX-5A, Kowloon Bay, Hong Kong). Before analyzing, a 1:2 dilution was created with a citrate–phosphate buffer of the appropriate pH value.

2.2.2.8.2 | Confocal Laser Scanning Microscopy. The microstructure of the solutions was also visualized using CLSM (C2+, Nikon, Tokyo, Japan) with a 40× objective. About 10 g kg^{-1} pea flour solutions were stained with Fluorescein-5-isothiocyanate (FITC) to visualize proteins, Nile red to visualize lipids, and calcofluor-white to visualize starch. The dyes were added to the solutions, mixed, and a drop of the stained solution was added to an object glass with a cover slip on top before analyzing. The different stains were visualized using lasers emitting light at wavelengths of 405 to 561 nm that resulted in colors of green, red, and blue for protein, lipids, and fiber, respectively.

2.2.3 | Visual Analysis

To visualize the sedimentation rate of the pea flour solutions, the solutions were photographed (EOS Rebel t7, Canon, New York, USA) in a lightbox after agitation ($t = 0$ min), after 30 min, and after 60 min.

2.2.4 | Statistical Analysis

All results generated were analyzed using RStudio (Version 2023.12.0 + 369, Posit Software, PBC, Boston, USA). All experiments were repeated at least twice, and each measurement was carried out at least in duplicate. ANOVA and post hoc tests using Tukey's method were performed with a p value of 0.05. The figures have been plotted in OriginPro (Version 2020).

3 | Results and Discussion

3.1 | Selection Process

The overall aim of this study was to reveal intrinsic differences between flours of selected pea accessions. The selected accessions span domestication levels from wild species to modern cultivars. Initially, 650 accessions were screened by collecting NIR spectra in the range of 400–2500 nm. The detector registers the intensity of the light at different wavelengths reflected from the sample, creating an absorbance spectrum illustrated in Figure 2.

Figure 2 illustrates that there is a spectral variation between samples as the absorption intensity at different wavelengths varies between samples. This is most likely correlated to the chemical composition of the sample measured as molecular bonds absorb at different wavelengths, resulting in a spectrum (Osborne 2000). The height of the peak (the absorption intensity) can be translated to the concentration of the molecules absorbing at a given wavelength by utilizing Lambert–Beer's law (Equation 2):

$$A = \epsilon_{\lambda} \cdot l \cdot c = -\log\left(\frac{I}{I_0}\right) \quad (2)$$

with A = absorbance, $\in_{\lambda}$ = extinction coefficient, l = path length the light travels in the sample, c = molar concentration in the sample, I_0 = path length from the light bulb to the sample, I = path length from the sample to the detector.

As Equation (2) indicates, if the extinction coefficient and the path length of the light are constant, the absorbance of light must be equal to the concentration in the sample (Sørensen et al. 2021). Due to the high signal-to-noise ratio present in the visual part of the spectra (400–750 nm) illustrated in Figure 2, this spectral range was excluded in the subsequent analysis.

PCA was performed to investigate the relationship between the samples. To reduce the signal-to-noise ratio and the baseline effect in the spectra, two pre-processing methods were applied to the spectral data: Standard Normal Variate and Mean Centering, and score (Figure 3), as well as loading plots (Figure S1) were prepared (Tomasi et al. 2004). The PCA loadings for both PC1 and PC2 are primarily influenced by variables in the 1900–2000 nm range, where combination bands of —OH and —NH_2 groups and the second overtone of —C═O absorption occur. These molecules are associated with water, protein, and fat, respectively. Both PC1 and PC2 also contain a pronounced peak around 1400 nm where the first overtone of —OH and —NH absorb. These molecules indicate starch and proteins present in the pea seeds (Osborne et al. 1993; Engineering 2013). The score plot was then used to reduce the number of samples but still showcase potential differences among the pea accessions. Twentyaccessions were selected based on their different locations within the score plot (Figure 3). It was anticipated that the rapid NIR screening would enable the detection of distinctions among a vast sample population, thereby facilitating the selection of unique samples for more detailed analysis.

The 20 chosen pea samples were analyzed for their compositional differences by reference methods. These results showed that the pea accessions were considerably different from each other, as illustrated in Table 1, indicating that the spectral differences are associated with compositional differences. For example, the protein content ranged from 173.2 to 256.9 g kg^{-1}, the lipid content from 12.1 to 30.2 g kg^{-1}, and the starch content from 338.5 to 501.4 g kg^{-1} (in dry matter). Moreover, they displayed distinct colors, primarily due to flavonoids present in their seed coats, which also influence the coloration of the resulting flour dispersions (Figure S2) (Ding Tao et al. 2023). Interestingly, it appears that the pH levels also influence the coloring properties of these flavonoids, which can exhibit color changes dependent on the pH in question. This is likely the reason for the observed differences in color across the various pH values tested (Stavenga et al. 2020). However, the seeds are often de-husked for industrial processing, and therefore, the color differences might not be that relevant for industrial applications.

Overall, NIR screening effectively identified compositionally distinct pea accessions. Whether these differences also translate to physicochemical and functional properties is explored in the following sections.

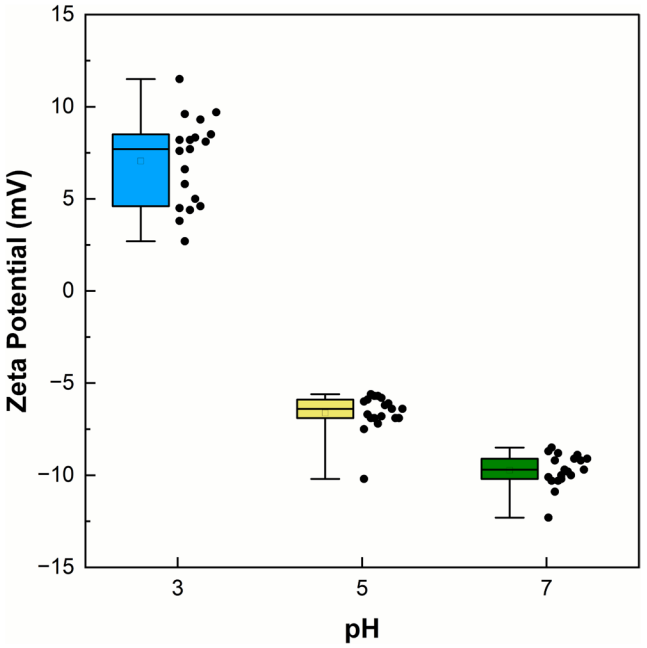


FIGURE 4 | Surface charge of 19 pea accessions at pH 3, 5, and 7. The results from NGB103523 were removed as they were classified as outliers influencing the distribution of the plot. Pea sample 9 was excluded because of extensive sedimentation in the measuring cell.

3.2 | Physicochemical Properties

3.2.1 | Surface Charge

Initially, the zeta potential of the solutions was measured as a function of pH. The zeta potential represents the electrical potential at the slipping plane and is an important parameter when characterizing the stability of a dispersed system (Cano-Sarmiento et al. 2018). The zeta potential is determined by the presence of charged compounds in the solution, which are often proteins, polysaccharides, and other ions (Tanger et al. 2020). The results of the zeta potential measurements are shown in Figure 4.

As expected, the zeta potential changed when the pH of the solution was adjusted. Proteins possess a pH-dependent surface charge, which depends on the number and location of the amino acid-specific residues. A positive charge was obtained for all samples at pH 3, which is in line with the reported isoelectric point of pea proteins at around 4.7–4.9 (Stone et al. 2015). Above the isoelectric point, all accessions exhibited a negative charge, with a more pronounced negative charge at pH 7 compared to pH 5. At both pH 5 and 7, the protein particles exhibited low negative electrostatic charge, which ranged from -5.6 ± 0.0 to -7.5 ± 0.9 mV and -8.5 ± 0.4 to -12.3 ± 3.3 mV, respectively. The charge variation between the accessions is relatively low at these pH values and is the sum of the different protein fractions (i.e., albumins and globulins), but also the polysaccharides present (such as pectin) in the samples can influence the measured charge (Tanger et al. 2020). The results of the zeta potential measurements at pH 3 exhibited a greater difference between pea accessions and ranged from 2.7 ± 1.4 to 11.5 ± 1.4 mV. At pH 3, the lowest zeta potential result was obtained from the wild pea accession NGB101787, while the highest result was obtained from the improved cultivar NGB13784.

Interestingly, the measured zeta potentials are quite low and would result in an unstable colloidal solution if no other repulsive mechanism is present. According to Cano-Sarmiento et al. (2018), it must be acknowledged that the measurements were performed on flour and that counterions present in the flour most likely reduced the measured net charge. However, other authors such as Lam (2016) reported no significant difference in surface charge between pea protein isolates obtained from different cultivars, and the zeta potential measurements in their study ranged from −23.0 to −24.3 mV at pH 7. These values were higher compared to the ones presented in Figure 4, which is most likely related to the extraction procedure, which results in an isolated protein ingredient with fewer countercharges present. Moreover, the protein extraction procedure can result in denaturation, which can cause a change in surface composition and ultimately also in the zeta

TABLE 2 | Enthalpy and peak temperatures obtained from the DSC analysis of the 20 pea accessions.

Pea sample	Pea accession	Enthalpy ΔH (J/g)	Peak I temperature (°C)	Enthalpy ΔH (J/g)	Peak II temperature (°C)
1	NGB102401	$1.75^{a} \pm 0.11$	$63.9^{j} \pm 0.17$	$0.13^{cdef} \pm 0.00$	$88.2^{bc} \pm 0.22$
2	NGB11935	$1.04^{abcde} \pm 0.01$	$64.9^{hij} \pm 0.44$	$0.06^{ef} \pm 0.02$	$87.3^{bc} \pm 0.04$
3	NGB20013	$1.36^{abcd} \pm 0.10$	$67.5^{def} \pm 0.39$	$0.05^{ef} \pm 0.02$	$85.4^{c} \pm 0.05$
4	NGB103830	$1.42^{abcd} \pm 0.23$	$66.6^{efgh} \pm 0.03$	$0.09^{def} \pm 0.03$	$87.0^{c} \pm 0.24$
5	NGB17833	$1.01^{bcde} \pm 0.06$	$67.9^{def} \pm 0.15$	$0.06^{ef} \pm 0.01$	$85.7^{c} \pm 0.18$
6	NGB8646	$1.15^{abcde} \pm 0.01$	$73.2^{b} \pm 0.11$	$0.04^{f} \pm 0.00$	$88.2^{bc} \pm 0.17$
7	NGB106016	$1.28^{abcd} \pm 0.14$	$68.7^{d} \pm 0.04$	$0.28^{ab} \pm 0.00$	$94.2^{a} \pm 0.24$
8	NGB105418	$1.15^{abcde} \pm 0.13$	$67.0^{defg} \pm 0.57$	$0.03^{f} \pm 0.01$	$86.9^{c} \pm 0.29$
9	NGB103523	$0.90^{de} \pm 0.04$	$68.9^{d} \pm 0.30$	$0.03^{f} \pm 0.00$	$85.7^{c} \pm 0.27$
10	NGB101787	$0.49^{e} \pm 0.10$	$64.7^{ij} \pm 0.07$	$0.21^{abcd} \pm 0.01$	$87.5^{bc} \pm 0.62$
11	NGB102149	$1.53^{abcd} \pm 0.28$	$68.2^{def} \pm 1.32$	$0.25^{abc} \pm 0.05$	$90.5^{b} \pm 3.54$
12	NGB20205	$0.82^{de} \pm 0.11$	$82.2^{a} \pm 0.45$	—	—
13	NGB17869	$1.70^{ab} \pm 0.17$	$66.4^{fghi} \pm 0.18$	$0.34^{a} \pm 0.11$	$88.6^{bc} \pm 0.11$
14	NGB102153	$0.92^{cde} \pm 0.17$	$72.8^{bc} \pm 0.32$	$0.09^{def} \pm 0.06$	$85.3^{c} \pm 0.02$
15	NGB102222	$1.02^{abcde} \pm 0.09$	$65.3^{ghij} \pm 0.33$	$0.34^{a} \pm 0.06$	$94.1^{a} \pm 0.16$
16	NGB24334	$1.09^{abcde} \pm 0.18$	$71.1^{c} \pm 0.67$	$0.18^{bcde} \pm 0.02$	$87.3^{bc} \pm 0.89$
17	NGB13784	$1.18^{abcde} \pm 0.34$	$68.1^{def} \pm 0.10$	$0.03^{f} \pm 0.00$	$85.2^{c} \pm 0.81$
18	NGB102680	$1.50^{abcd} \pm 0.04$	$67.1^{defg} \pm 0.34$	$0.09^{def} \pm 0.02$	$88.2^{bc} \pm 0.14$
19	NGB103050	$1.64^{abc} \pm 0.35$	$67.6^{def} \pm 0.73$	$0.12^{cdef} \pm 0.02$	$87.0^{c} \pm 0.60$
20	NGB100005	$1.70^{ab} \pm 0.30$	$68.4^{de} \pm 0.15$	$0.01^{f} \pm 0.01$	$86.8^{c} \pm 0.74$

Note: Different lower-case superscripts indicate statistically significant differences in the same column ($p < 0.05$); (—) no peak identified.

potential (Tanger et al. 2020). However, the results presented in Figure 4 indicate that the zeta potential does differ between pea accessions with proteins in their native state, especially in the lower acidic pH range. This can influence the stability of colloidal solutions or dispersions stabilized with these proteins because a high electrostatic repulsion can stabilize a colloidal system, whereas a low electrostatic repulsion is preferred for gelation or controlled aggregation (Masia et al. 2022).

3.2.2 | Thermal Properties

DSC analysis was used to obtain the enthalpy of phase transition and the temperature at which these transitions occur. It was expected that especially the starch gelation and the protein denaturation would impact the measured transitions. The results of the thermal analysis are reported in Table 2, and to further illustrate the differences, the DSC curves of five selected pea accessions that show distinctive differences were plotted in Figure 5.

All accessions except for NGB20205 yielded two peaks. The first peak had temperatures from 63.9°C ± 0.2°C to 73.2°C ± 0.2°C for the 20 different accessions, which is most likely related to the gelatinization of starch. The second peak exhibited an even broader range with peak temperatures ranging from 85.2°C ± 0.2°C to 94.2°C ± 0.24°C. This peak can be attributed to the denaturation of protein. However, it must be considered that the measured flour is a complex matrix and that the observed peaks could be the result of multiple components and their interactions (Parniakov et al. 2018). For example, Hall and Moraru (2021) measured untreated pea protein concentrate and found a phase transition that was related to amylose-lipid complexes at around $T = 94$°C. This complex might explain the third peak observed in some of the curves. Moreover, the reported protein denaturation values in this study are slightly higher compared to previously reported denaturation temperatures for pea proteins (Mession et al. 2015). It must be considered that these values are typically obtained from isolated protein fractions that undergo extensive extraction and drying processes before the measurements. The refinement typically includes a dialysis step that removes ions that are known to increase the denaturation temperature (Mession et al. 2013). In contrast, the samples in the present study were measured as is and without a drying operation. To confirm that the observed peaks can be associated with starch gelation and protein denaturation, the starch and protein fractions were separated and individually measured under the same conditions. The DSC measurements of the separated starch and protein fractions did indeed confirm that the peaks illustrated in Figure 5 can be attributed to the gelatinization of starch (Peak 1) and denaturation of proteins (Peak 2) (see Table S2 in the Appendix).

Interestingly, the DSC curve derived for NGB20205 differed from the other pea accessions, as shown in Figure 5. When heated, this accession displayed only one peak from $T = 63$ to 94°C. This might be related to the lobed structure of the starch granules, which is illustrated in Figure 8. It was previously

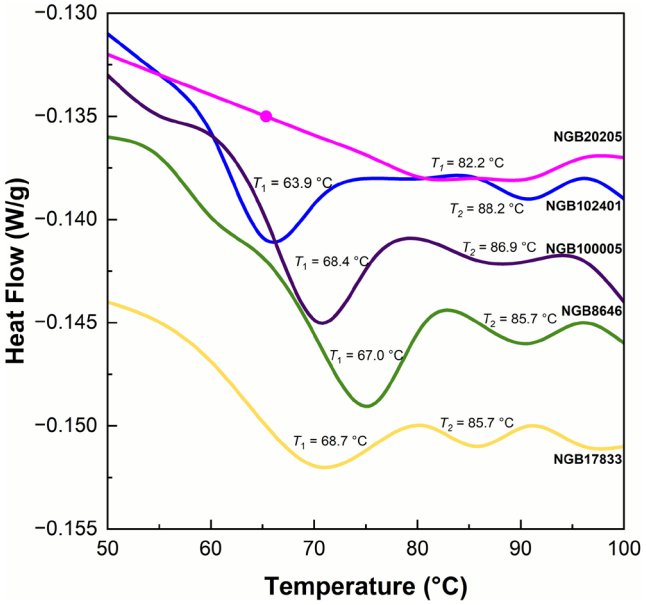


FIGURE 5 | Endothermic peaks and transition temperatures of five selected pea accessions to showcase the distinctive differences between them. See Table 2 for thermal peaks for all accessions.

TABLE 3 | Surface and volume-based mean particle size measured by static light scattering of flours obtained from the 20 pea accessions.

Pea sample	Pea accession	$D_{3,2}$ (μm)	$D_{4,3}$ (μm)	Span
1	NGB102401	$20.9^{fg} \pm 0.2$	$56.6^{h} \pm 1.8$	4.0
2	NGB11935	$11.5^{a} \pm 0.1$	$24.6^{cd} \pm 0.8$	2.6
3	NGB20013	$18.0^{bc} \pm 0.3$	$76.8^{b} \pm 3.5$	6.3
4	NGB103830	$14.3^{e} \pm 0.9$	$43.6^{ef} \pm 4.9$	3.8
5	NGB17833	$13.5^{e} \pm 0.2$	$40.6^{fg} \pm 1.3$	4.1
6	NGB8646	$13.4^{e} \pm 0.4$	$42.4^{f} \pm 1.6$	4.7
7	NGB106016	$14.2^{e} \pm 0.2$	$40.1^{fg} \pm 1.4$	3.4
8	NGB105418	$16.3^{d} \pm 0.3$	$52.6^{de} \pm 1.5$	3.7
9	NGB103523	$9.5^{hi} \pm 0.1$	$38.5^{fg} \pm 0.9$	3.8
10	NGB101787	$11.7^{f} \pm 0.4$	$45.8^{ef} \pm 7.2$	4.9
11	NGB102149	$17.7^{c} \pm 0.4$	$72.0^{b} \pm 2.3$	6.0
12	NGB20205	$9.5^{hi} \pm 0.2$	$39.8^{fg} \pm 0.7$	4.8
13	NGB17869	$20.9^{a} \pm 0.2$	$95.4^{a} \pm 2.7$	6.6
14	NGB102153	$8.8^{i} \pm 0.2$	$40.9^{fg} \pm 0.5$	4.5
15	NGB102222	$18.1^{bc} \pm 0.6$	$76.8^{b} \pm 4.9$	5.3
16	NGB24334	$15.6^{d} \pm 0.2$	$79.9^{b} \pm 2.1$	7.3
17	NGB13784	$19.0^{b} \pm 0.4$	$89.7^{a} \pm 1.9$	36.2
18	NGB102680	$10.5^{gh} \pm 0.3$	$32.2^{g} \pm 1.5$	5.4
19	NGB103050	$18.4^{bc} \pm 0.2$	$62.9^{c} \pm 2.6$	4.8
20	NGB100005	$7.1^{j} \pm 0.1$	$38.6^{fg} \pm 1.1$	4.2

Note: Different lower-case superscripts indicate statistically significant differences in the same column ($p < 0.05$).

reported that this starch structure has a low gelatinization enthalpy and onset temperature that is more similar to broken starch granules (Ashogbon et al. 2021). This might explain why the curve only consists of one wide peak, possibly derived from the phase transition of starch and protein collectively.

The large differences in gelation and denaturation temperatures can have important consequences for food applications in which thermal stability is an important parameter. The limited thermal stability of starch, for instance, results in the formation of a gel at temperatures well below those required for protein denaturation. Forming a gel at low temperatures can help maintain the functionality and structural integrity of the proteins within the starch gel matrix. On the other hand, pea flour with high thermal stability will be able to withstand pasteurization, which is a widely used processing step to ensure microbial-safe food products.

3.2.3 | Particle Size

The particle size of the different compounds in pea flour is an important parameter that determines a variety of different properties, such as solubilization, sedimentation, light scattering, and thickening (Khushbu and Sunil 2020). Table 3 illustrates the results obtained from the 20 pea accessions measured at pH 7. The surface mean diameter of the particles ranges between 7.1 ± 0.1 and 20.9 ± 0.2 μm. When compared to the pictures obtained through CLSM visualization (Figure 8), it can be concluded that these measurements most likely reflect mainly the size of the starch granules in the solution. The typical size of a pea starch granule is between 2 and 40 μm, while the size of the protein bodies ranges between 1 and 3 μm (Sridharan et al. 2020). The results indicate that despite the same milling conditions being used for all pea accessions, the particle size of the pea flour differs significantly. This may have important consequences for processing pea flours since it can be expected that the sedimentation and viscosity are different for the individual pea flours, which impacts their processability.

3.3 | Functional Properties

3.3.1 | Protein Solubility

Protein solubility is an important parameter in food applications since it determines whether a protein remains in a solution under specific conditions. Solubilized proteins can diffuse to interfaces, whereas insoluble proteins precipitate and may form aggregates or gelled matrices (Zhao et al. 2020). Protein solubility is therefore an important functional property for determining the suitability of an ingredient to be used in food applications.

Figure 6 illustrates the protein solubility at pH 3, 5, and 7. A clear variation between pea accessions is displayed at all pH values, but is most pronounced at pH 7. Interestingly, the solubility at pH 3 and 5 has similar variations from 13.8% ± 1.8% (NGB101787) to 53.4% ± 11.9% (NGB24334) and 19.3% ± 0.9% (NGB101787) to 56.5% ± 7.4% (NGB24334), respectively. The range at pH 7 is considerably higher, with solubilities ranging from 29.8% ± 6.0% (NGB102222) to 94.8% ± 1.1% (NGB17833).

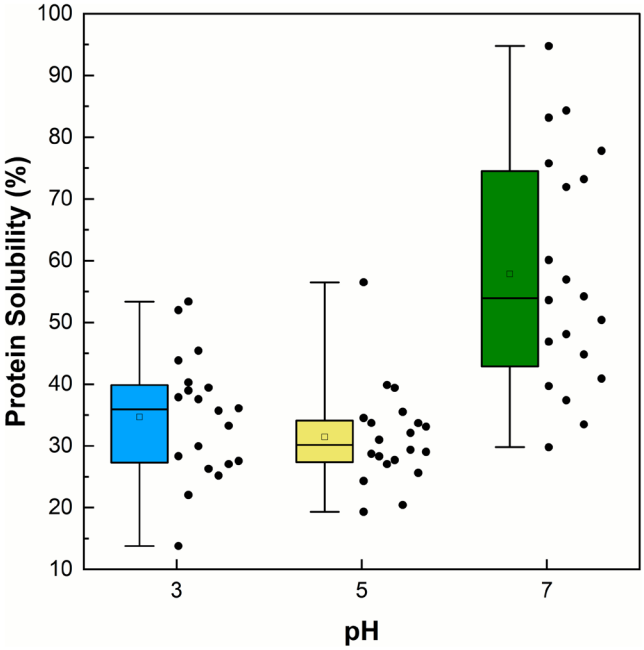


FIGURE 6 | Protein solubility presented as a ratio of protein concentration in supernatant to total protein concentration of 20 pea accessions at pH 3, 5, and 7.

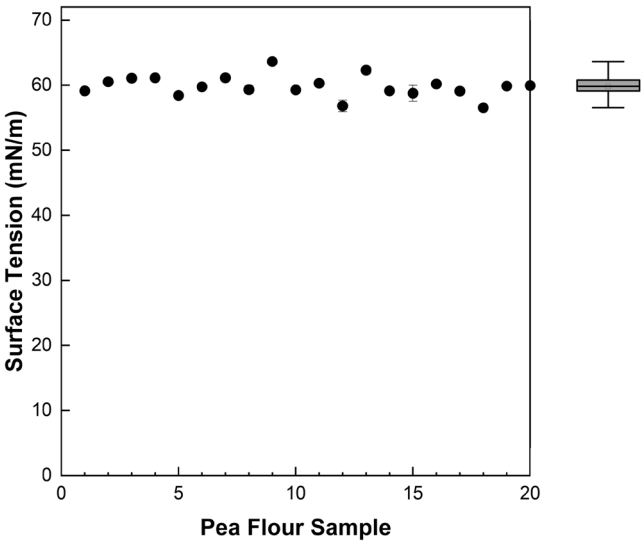


FIGURE 7 | Dynamic surface tension of the 20 pea accessions at a flour concentration of 1%.

This displays the impact of intrinsic characteristics on the functional properties of pea proteins. This may be due to various factors, including intrinsic differences in amino acid composition or variations in phytic acid content, which has been shown to interact with proteins, particularly under conditions below their isoelectric point (Amat et al. 2024). Low solubilities of pea proteins could be overcome by selecting the right accessions, as shown in these results. Within the same plant species, the solubility can vary by more than 60% before any processing has been carried out, but pH-driven changes in solubility can be attenuated by selecting the right accession. For example, accession NGB24334 exhibits a solubility of 60.2% ± 7.6% at pH 3, but only 39.4% ± 6.7% at pH 7, whereas NGB17869 has a solubility of

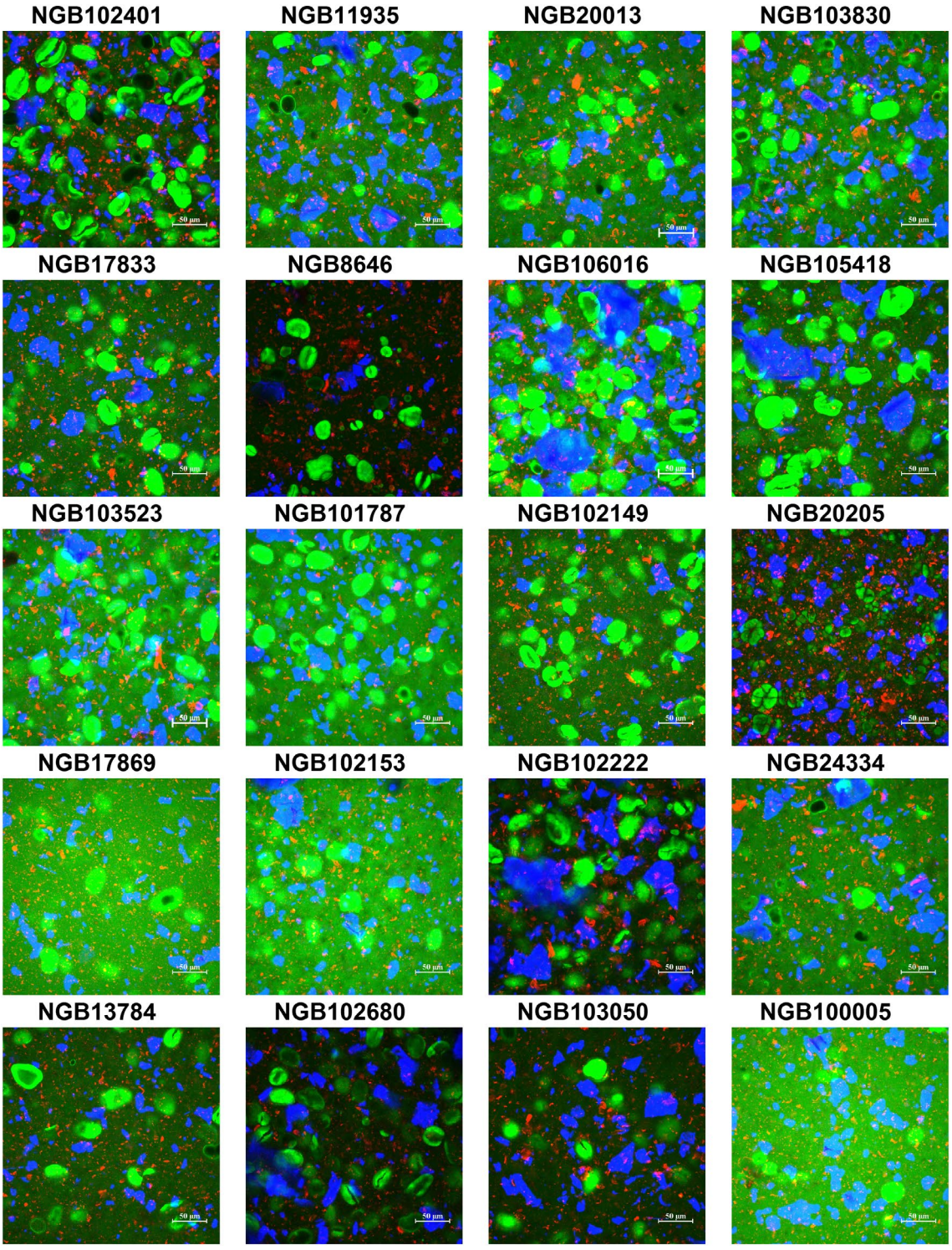


FIGURE 8 | Microstructure of 20 pea accessions at pH 7 visualized through confocal laser scanning microscopy. The green stain indicates proteins (mainly around the starch granules), blue indicates fiber, and red indicates lipids. Scale bar 50 μm.

92.2% ± 1.5% at pH 7 but only 29.6% ± 1.2% at pH 3. Thus, careful selection of the accession will be required in the future to ensure optimum functionality.

However, the ideal solubility varies depending on the application. A high solubility at pH 7 could be optimal for producing pea protein milk alternatives, whereas a low solubility at pH 3 is needed for acid-gelling applications. Therefore, choosing a pea accession with the desired solubility at the desired pH plays an important role in product development. It has to be mentioned that the reported solubilities are for the native states of the protein, and it is known that heat treatment can decrease the solubility due to protein denaturation and increased surface hydrophobicity (Hall and Moraru 2021). Therefore, further studies are needed to investigate whether the observed differences remain even after such processing operations.

3.3.2 | Interfacial Tension

Many proteins are surface-active and can lower the surface tension by adsorbing and unfolding at the interface to optimize the exposure of their functional groups to the different phases (Sridharan et al. 2020). The speed of the reduction of the interfacial tension influences the stability of, for example, the foam created (Moll et al. 2019). The dynamic surface tension was therefore measured for the flours obtained from the different pea accessions, and the results are shown in Figure 7.

The results indicate that the pea accessions behave differently when interacting with the liquid/air interface. NGB20205 and NGB102680 exhibit a significantly lower dynamic surface tension (Figure S3), indicating an increased surface activity compared to the other pea accessions (McClements 2016). In contrast, NGB103523 and NGB17869 exhibit significantly less favorable interfacial properties, suggesting a lower presence of surface-active compounds available to stabilize the liquid–air interface, leading to increased surface tension. This could be related to two different phenomena. First, the measurements were carried out at a constant flour concentration to account for other potential surface-active compounds besides proteins. However, the employed flours have different protein contents, which could affect the measured results (Table 1). Some authors choose a constant protein or surface-active compound to perform such measurements, but in crude flour, many surface-active compounds are present, which is why a constant dry matter was chosen in the present study (Guraya et al. 2025). Nonetheless, higher protein contents did not necessarily result in a lower interfacial tension. For example, the pea accessions NGB17869 (pea sample 13) and NGB102680 (pea sample 18) both contain 23.3 g kg^{-1} protein but exhibit significantly different interfacial properties. Second, the molecular composition and structure of the proteins in the flour might differ, which can impact their ability to interact with the interface and lower the surface tension. This shows that an optimum relationship between protein content and protein composition is required to achieve the desired interfacial activity.

3.4 | Microstructure

These measurements were carried out to visualize the microstructural differences between the different pea accessions, as illustrated in Figure 8, and the corresponding light microscopy images are shown in Table S3. CLSM images visually confirmed a variation in protein solubility at pH 7. The images obtained for NGB17869 and NGB100005 were dominated by the green color caused by the protein stain (FITC), and these two accessions also had high solubilities of 92.2% and 81.7%, respectively (Figure 6). On the contrary, NGB8646 and NGB102222 displayed lower solubilities of 55.7% and 28.4%, respectively, and exhibited a distinct microstructure where the proteins were predominantly located around the starch granules. According to Möller et al. (2021), Linskens et al. (1985), and Pernollet (1978), the starch granules are embedded in a matrix of protein bodies in the pea plant cell. Milling usually disrupts this structure, but the protein bodies readhere to the surface of the starch granules during the milling process (Möller et al. 2021). However, it has also been reported that starch granules can be naturally coated with proteins from the chloroplasts or amyloplasts in which they form, and that the observed protein layer may represent a combination of this native coating and additional deposits introduced during the milling process (Ma et al. 2018; Sharma et al. 2024). This accounts for the green staining of the starch granules, as the fluorescent dye binds to proteins present on their surfaces.

Another interesting observation is related to the accession NGB20205. It is classified as "rough/wrinkled," also known as compound granules, caused by a genetic mutation that results in reduced activity of the starch-branching enzyme. This leads to a higher amylose content compared to pea seeds without this mutation (Hedley et al. 2002; Ren et al. 2021). This genetic mutation can result in a lobed structure with multiple sub-granules within one starch granule, as visualized in the CLSM photo of NGB20205.

The blue-stained particles are insoluble fibers from the cell walls of the cotyledon and the hulls, and the red-stained particles are lipids. The size and the distribution of these particles also differ between pea accessions. Especially the presence of lipids in some of the accessions is noteworthy. Usually, peas are cultivated for their starch content, and lipids are not a compound of interest. Despite this, some of the accessions used in this study do contain lipids (Table 1), which is also showcased in the CLSM images. This can have a profound effect on the flavor of the pea flour because it is known that especially lipid oxidation in pulse-based ingredients can result in the formation of volatile off-flavors that decrease consumer acceptance (Roland et al. 2016).

4 | Conclusion

This study demonstrates that rapid NIR-based screening can effectively identify pea accessions with diverse intrinsic physicochemical and functional traits. The substantial variability observed among unrefined pea flours highlights the importance of accession selection to optimize ingredient functionality in whole-flour and fractionated compounds. The results presented in this study show that physicochemical and functional properties differ between pea accessions with great potential for the food industry. Accessions with a high protein solubility are good candidates for further screening to evaluate how processing affects the solubility and interfacial properties, whereas accessions with low thermal transitions are interesting for gelling applications at low temperatures. It can be concluded that a pea is not a pea and that careful selection of the accession is required to maximize the benefit of pea flour and derived ingredients in different food applications. Beyond accession selection, composition and functionality are also influenced by growing conditions and processing, and further studies as well as field trials are needed to elucidate these effects, particularly by investigating the physicochemical and functional properties of refined fractions and understanding how processing alters them.

Author Contributions

All authors conceived and designed the study. E.D.M. and L.G. wrote the first draft of the manuscript. E.D.M. carried out the research. E.D.M. and L.G. analyzed the data. All authors contributed to and approved the final draft of the manuscript.

Acknowledgments

Emma Dreyer Matzen acknowledges travel funding from FOSS Analytical. NordGen is greatly acknowledged for sharing pea seed materials used in this study.

Funding

This work is supported by the Agriculture and Food Research Initiative—Foundational and Applied Science Program, project award no. 2022-67017-36597 from the US Department of Agriculture's National Institute of Food and Agriculture. Any opinions, findings, conclusions, or recommendations expressed in this publication are those of the author(s) and should not be construed to represent any official USDA or US Government determination or policy. In addition, this material is based upon work supported by the National Institute of Food and Agriculture, U.S. Department of Agriculture, and the Food Science Department at University of Massachusetts Amherst, under project number MAS00612.

Ethics Statement

No humans or animals were used in this research.

Conflicts of Interest

E.D.M. and M.S.M. are employed by FOSS. Their employment did not influence the design, execution, or interpretation of this study.

References

Amat, T., A. Assifaoui, J. Buczkowski, J. V. C. Silva, C. Schmitt, and R. Saurel. 2024. "Interplay Between Soluble and Insoluble Protein/Calcium/Phytic Acid Complexes in Dispersions of Faba Bean and Pea Protein Concentrates Around Neutral pH." *Food Hydrocolloids* 147: 109273. https://doi.org/10.1016/j.foodhyd.2023.109273.

Ashogbon, A. O., E. T. Akintayo, A. O. Oladebeye, A. D. Oluwafemi, A. F. Akinsola, and O. E. Imanah. 2021. "Developments in the Isolation, Composition, and Physicochemical Properties of Legume Starches." *Critical Reviews in Food Science and Nutrition* 61, no. 17: 2938–2959. https://doi.org/10.1080/10408398.2020.1791048.

Bro, R., and A. K. Smilde. 2014. "Principal Component Analysis." *Analytical Methods* 6, no. 9: 2812–2831. https://doi.org/10.1039/c3ay41907j.

Cano-Sarmiento, C., D. I. Téllez-Medina, R. Viveros-Contreras, et al. 2018. "Zeta Potential of Food Matrices." *Food Engineering Reviews* 10, no. 3: 113–138. https://doi.org/10.1007/s12393-018-9176-z.

Chao, D., and R. E. Aluko. 2018. "Modification of the Structural, Emulsifying, and Foaming Properties of an Isolated Pea Protein by Thermal Pretreatment." *CyTA—Journal of Food* 16, no. 1: 357–366. https://doi.org/10.1080/19476337.2017.1406536.

Chen, S. K., H. F. Lin, X. Wang, Y. Yuan, J. Y. Yin, and X. X. Song. 2023. "Comprehensive Analysis in the Nutritional Composition, Phenolic Species and In Vitro Antioxidant Activities of Different Pea Cultivars." *Food Chemistry: X* 17: 100599. https://doi.org/10.1016/j.fochx.2023.100599.

Choi, H., M. Taghvaei, B. Smith, and G. M. Ganjyal. 2022. "Biochemical Analysis of Protein Compositions Among Pea (*Pisum sativum*) Cultivars Grown in the Northwest USA." *ACS Food Science & Technology* 2, no. 7: 1067–1076. https://doi.org/10.1021/acsfoodscitech.1c00460.

Ding Tao, W., W.-X. Li, J.-J. Wan, Y.-C. Hu, R.-Y. Gan, and L. Zou. 2023. "A Comprehensive Review of Pea (*Pisum sativum* L.): Chemical Composition, Processing, Health Benefits, and Food Applications." *Food* 12: 2527. https://doi.org/10.3390/foods12132527.

Engineering, N. I. 2013. "Near-IR Absorption Bands." www.ndc.com.

FAO. 2018. *Dry Peas Production*. World Mapper.

FOSS Analytical. 2018a. "Hydrotec™ 8000."

FOSS Analytical. 2018b. "Soxtec™ 8000."

FOSS Analytical. 2019. "Dumatec™ 8000."

François Mariotti, D. D. T., and P. P. Mirand. 2008. "Converting Nitrogen Into Protein—Beyond 6.25 and Jones' Factors." *Food Science & Nutrition* 48: 177–184.

Garcia Arteaga, V., S. Kraus, M. Schott, I. Muranyi, U. Schweiggert-Weisz, and P. Eisner. 2021. "Screening of Twelve Pea (*Pisum sativum* L.) Cultivars and Their Isolates Focusing on the Protein Characterization, Functionality, and Sensory Profiles." *Food* 10, no. 4: 40758. https://doi.org/10.3390/foods10040758.

Grossmann, L. 2023. "Structural Properties of Pea Proteins (*Pisum sativum*) for Sustainable Food Matrices." *Critical Reviews in Food Science and Nutrition* 64: 8346–8366. https://doi.org/10.1080/10408398.2023.2199338.

Guillin, F. M., C. Gaudichon, L. Guerin-Deremaux, et al. 2022. "Real Ileal Amino Acid Digestibility of Pea Protein Compared to Casein in Healthy Humans: A Randomized Trial." *American Journal of Clinical Nutrition* 115, no. 2: 353–363. https://doi.org/10.1093/ajcn/nqab354.

Guraya, M. A., C. Accoroni, M. A. Espósito, P. A. Torresi, M. A. Reinheimer, and E. Godoy. 2025. "Impact of Solid-State Fermentation With Aspergillus Niger on the Chemical Composition of Yellow Pea (*Pisum sativum* L.) Flour and Its Application for Obtaining Protein Products. ACS." *Food Science and Technology* 5, no. 7: 2763–2775. https://doi.org/10.1021/acsfoodscitech.5c00237.

Hall, A. E., and C. I. Moraru. 2021. "Structure and Function of Pea, Lentil and Faba Bean Proteins Treated by High Pressure Processing and Heat Treatment." *Lwt* 152: 112349. https://doi.org/10.1016/j.lwt.2021.112349.

Hansen, L., F. Bu, and B. P. Ismail. 2022. "Structure-Function Guided Extraction and Scale-Up of Pea Protein Isolate Production." *Food* 11, no. 23: 33773. https://doi.org/10.3390/foods11233773.

Hedley, C. L., T. Y. Bogracheva, and T. L. Wang. 2002. "A Genetic Approach to Studying the Morphology, Structure and Function of Starch Granules Using Pea as a Model." *Starch—Stärke* 54, no. 6: 235–242. https://doi.org/10.1002/1521-379x(200206)54:6<235::Aid-star235>3.0.Co;2-r.

ICC. 1990. "104/1 Determination of Ash in Cereals and Cereal Products."

Khushbu, S., and C. K. Sunil. 2020. "Effect of Particle Size, Concentration, Temperature and pH on Rheological Properties of Shallots Flour." *Journal of Food Science and Technology* 57, no. 10: 3601–3610. https://doi.org/10.1007/s13197-020-04392-8.

Kotlarz, A., A. Sujak, W. Strobel, and W. Grzesiak. 2011. "Chemical Composition and Nutritive Value of Protein of the Pea Seeds—Effect of Harvesting Year and Variety." *Journal of Fruit and Ornamental Plant Research* 75, no. 1: 57–69. https://doi.org/10.2478/v10032-011-0018-2.

Lam, A. C. Y. 2016. *Effect of Cultivar and Environment on the Physicochemical and Functional Properties of Pea Protein Isolates Saskatchewan*. College of Graduate Studies and Research.

Lam, A. C. Y., T. D. Warkentin, R. T. Tyler, and M. T. Nickerson. 2016. "Physicochemical and Functional Properties of Protein Isolates Obtained From Several Pea Cultivars." *Cereal Chemistry* 94, no. 1: 89–97. https://doi.org/10.1094/cchem-04-16-0097-fi.

Lie-Piang, A., N. Braconi, R. M. Boom, and A. van der Padt. 2021. "Less Refined Ingredients Have Lower Environmental Impact—A Life Cycle Assessment of Protein-Rich Ingredients From Oil- and Starch-Bearing Crops." *Journal of Cleaner Production* 292: 126046. https://doi.org/10.1016/j.jclepro.2021.126046.

Linskens, H. F. J., H.-F. Linskens, B. Anderson, et al. 1985. *Cell Components*. Vol. 1. Springer.

Liu, X., C. Yang, J. Qin, J. Li, J. Li, and J. Chen. 2023. "Challenges, Process Technologies, and Potential Synthetic Biology Opportunities for Plant-Based Meat Production." *Lwt* 184: 115109. https://doi.org/10.1016/j.lwt.2023.115109.

Ma, D., X. Huang, J. Hou, et al. 2018. "Quantitative Analysis of the Grain Amyloplast Proteome Reveals Differences in Metabolism Between Two Wheat Cultivars at Two Stages of Grain Development." *BMC Genomics* 19, no. 1: 768. https://doi.org/10.1186/s12864-018-5174-z.

Masia, C., P. E. Jensen, I. L. Petersen, and P. Buldo. 2022. "Design of a Functional Pea Protein Matrix for Fermented Plant-Based Cheese." *Food* 11, no. 2: 178. https://doi.org/10.3390/foods11020178.

McClements, D. J. 2016. *Food Emulsions: Principles, Practices, and Techniques*. 3rd ed. CRC Press.

Megazyme. 2024. *Total Starch (α-Amylase/Amyloglucosidase) Assay Protocol (K-TSTA-100A)*. Neogen Corporation. https://prod-docs.megazyme.com/documents/Assay_Protocol/K-TSTA-100A_DATA.pdf.

Mertens, C., L. Dehon, A. Bourgeois, C. Verhaeghe-Cartrysse, and C. Blecker. 2012. "Agronomical Factors Influencing the Legumin/Vicilin Ratio in Pea (*Pisum sativum* L.) Seeds." *Journal of the Science of Food and Agriculture* 92, no. 8: 1591–1596. https://doi.org/10.1002/jsfa.4738.

Message, J. L., N. Sok, A. Assifaoui, and R. Saurel. 2013. "Thermal Denaturation of Pea Globulins (*Pisum sativum* L.)-Molecular Interactions Leading to Heat-Induced Protein Aggregation." *Journal of Agricultural and Food Chemistry* 61, no. 6: 1196–1204. https://doi.org/10.1021/jf303739n.

Message, J.-L., M. L. Chihi, N. Sok, and R. Saurel. 2015. "Effect of Globular Pea Proteins Fractionation on Their Heat-Induced Aggregation and Acid Cold-Set Gelation." *Food Hydrocolloids* 46: 233–243. https://doi.org/10.1016/j.foodhyd.2014.11.025.

Moll, P., L. Grossmann, I. Kutzli, and J. Weiss. 2019. "Influence of Energy Density and Viscosity on Foam Stability—A Study With Pea Protein (*Pisum sativum* L.)." *Journal of Dispersion Science and Technology* 41, no. 12: 1789–1796. https://doi.org/10.1080/01932691.2019.1635028.

Möller, A. C., A. van der Padt, and A. J. van der Goot. 2021. "From Raw Material to Mildly Refined Ingredient—Linking Structure to Composition to Understand Fractionation Processes." *Journal of Food Engineering* 291: 110321. https://doi.org/10.1016/j.jfoodeng.2020.110321.

Osborne, B. G. 2000. "Near-Infrared Spectroscopy in Food Analysis." In *Encyclopedia of Analytical Chemistry*. Academic Press. https://doi.org/10.1002/9780470027318.a1018.

Osborne, B. G., T. Fearn, and P. H. Hindle. 1993. "In Practical NIR Spectroscopy With Applications in Food and Beverage Analysis." 2.

Parniakov, O., O. Bals, F. J. Barba, V. Mykhailyk, N. Lebovka, and E. Vorobiev. 2018. "Application of Differential Scanning Calorimetry to Estimate Quality and Nutritional Properties of Food Products." *Critical Reviews in Food Science and Nutrition* 58, no. 3: 362–385. https://doi.org/10.1080/10408398.2016.1180502.

Pernollet, J.-C. 1978. "Protein Bodies of Seeds: Ultra Protein Bodies of Seeds: Ultrastructure, Biochemistry, Biosynthesis and Degradation." *Phytochemistry* 17, no. 9: 1473–1480.

Ren, Y., T. Z. Yuan, C. M. Chigwedere, and Y. Ai. 2021. "A Current Review of Structure, Functional Properties, and Industrial Applications of Pulse Starches for Value-Added Utilization." *Comprehensive Reviews in Food Science and Food Safety* 20, no. 3: 3061–3092. https://doi.org/10.1111/1541-4337.12735.

Rex, M. C., D. C. E. Dawson, W. H. Elliott, and K. M. Jones. 1989. *Data for Biochemical Research*. 3rd ed. CABI Databases.

Roland, W. S. U., L. Pouvreau, J. Curran, F. van de Velde, and P. M. T. de Kok. 2016. "Flavor Aspects of Pulse Ingredients." *Cereal Chemistry* 94, no. 1: 58–65. https://doi.org/10.1094/cchem-06-16-0161-fi.

Santos, C. S., B. Carbas, A. Castanho, et al. 2019. "Variation in Pea (*Pisum sativum* L.) Seed Quality Traits Defined by Physicochemical Functional Properties." *Food* 8, no. 11: 10570. https://doi.org/10.3390/foods8110570.

Shand, P. J., H. Ya, Z. Pietrasik, and P. K. J. P. D. Wanasundara. 2007. "Physicochemical and Textural Properties of Heat-Induced Pea Protein Isolate Gels." *Food Chemistry* 102, no. 4: 1119–1130. https://doi.org/10.1016/j.foodchem.2006.06.060.

Sharma, M., M. R. Abt, S. Eicke, et al. 2024. "MFP1 Defines the Subchloroplast Location of Starch Granule Initiation." *Proceedings of the National Academy of Sciences of the United States of America* 121, no. 3: e2309666121. https://doi.org/10.1073/pnas.2309666121.

Sørensen, K. M., F. van den Berg, and S. B. Engelsen. 2021. "NIR Data Exploration and Regression by Chemometrics—A Primer." In *Near-Infrared Spectroscopy*, 127–189. Springer. https://doi.org/10.1007/978-981-15-8648-4_7.

Sridharan, S., M. B. J. Meinders, J. H. Bitter, and C. V. Nikiforidis. 2020. "Pea Flour as Stabilizer of Oil-in-Water Emulsions: Protein Purification Unnecessary." *Food Hydrocolloids* 101: 105533. https://doi.org/10.1016/j.foodhyd.2019.105533.

Stavenga, D. G., H. L. Leertouwer, B. Dudek, and C. J. van der Kooi. 2020. "Coloration of Flowers by Flavonoids and Consequences of pH Dependent Absorption." *Frontiers in Plant Science* 11: 600124. https://doi.org/10.3389/fpls.2020.600124.

Stone, A. K., N. A. Avarmenko, T. D. Warkentin, and M. T. Nickerson. 2015. "Functional Properties of Protein Isolates From Different Pea Cultivars." *Food Science and Biotechnology* 24, no. 3: 827–833. https://doi.org/10.1007/s10068-015-0107-y.

Taghvaei, M., R. Sadeghi, and B. Smith. 2022. "Seed to Seed Variation of Proteins of the Yellow Pea (*Pisum sativum* L.)." *PLoS One* 17, no. 8: e0271887. https://doi.org/10.1371/journal.pone.0271887.

Tanger, C., J. Engel, and U. Kulozik. 2020. "Influence of Extraction Conditions on the Conformational Alteration of Pea Protein Extracted From Pea Flour." *Food Hydrocolloids* 107: 105949. https://doi.org/10.1016/j.foodhyd.2020.105949.

Tomasi, G., F. van den Berg, and C. Andersson. 2004. "Correlation Optimized Warping and Dynamic Time Warping as Preprocessing Methods for Chromatographic Data." *Journal of Chemometrics* 18, no. 5: 231–241. https://doi.org/10.1002/cem.859.

Vidal-Valverde, C., J. Frias, A. Hernández, et al. 2003. "Assessment of Nutritional Compounds and Antinutritional Factors in Pea (*Pisum sativum*) Seeds." *Journal of the Science of Food and Agriculture* 83, no. 4: 298–306. https://doi.org/10.1002/jsfa.1309.

Zhao, H., C. Shen, Z. Wu, Z. Zhang, and C. Xu. 2020. "Comparison of Wheat, Soybean, Rice, and Pea Protein Properties for Effective Applications in Food Products." *Journal of Food Biochemistry* 44, no. 4: e13157. https://doi.org/10.1111/jfbc.13157.

Supporting Information

Additional supporting information can be found online in the Supporting Information section. **Data S1:** sfp270051-sup-0001-Supinfo.docx.